Original Article

A computer vision model for the identification and scoring of calcium in aortic valve stenosis: a single-center experience

Tibor Poruban, Dominik Pella, Ingrid Schusterova, Marta Jakubova, Karolina Angela Sieradzka Uchnar, Marianna Barbierik Vachalcova

East Slovak Institute of Cardiovascular Diseases and School of Medicine, Pavol Jozef Safarik University, Kosice, Slovakia

Contributions: (I) Conception and design: T Poruban; (II) Administrative support: I Schusterova; (III) Provision of study materials or patients: All authors; (IV) Collection and assembly of data: T Poruban, D Pella; (V) Data analysis and interpretation: T Poruban; (VI) Manuscript writing: All authors; (VII) Final approval of manuscript: All authors.

Correspondence to: Dominik Pella, MD, PhD. East Slovak Institute of Cardiovascular Diseases and School of Medicine, Pavol Jozef Safarik University, Ondavska 8, Kosice, Slovakia. Email: dominik.pella@gmail.com.

Background: Echocardiography is widely used to assess aortic stenosis (AS) but can yield inconsistent results, leading to uncertainty about AS severity and the need for further diagnostics. This retrospective study aimed to evaluate a novel echocardiography-based marker, the signal intensity coefficient (SIC), for its potential in accurately identifying and quantifying calcium in AS, enhancing noninvasive diagnostic methods.

Methods: Between May 2022 and October 2023, 112 cases of AS that were previously considered severe by echocardiography were retrospectively evaluated, as well as a group of 50 cases of mild or moderate AS, both at the Eastern Slovak Institute of Cardiovascular Diseases in Kosice, Slovakia. Utilizing ImageJ software, we quantified the SIC based on ultrasonic signal intensity distribution at the aortic valve's interface. Pixel intensity histograms were generated to measure the SIC, and it was compared with echocardiographic variables. To account for variations in brightness due to differing acquisition settings in echocardiography images (where the highest intensity corresponds to calcium), adaptive image binarization has been implemented. Subsequently, the region of interest (ROI) containing calcium was interactively selected and extracted. This process enables the calculation of a calcium pixel count, representing the spatial quantity of calcium. This study employed multivariate logistic regression using backward elimination and stepwise techniques. Receiver operating characteristic (ROC) curves were utilized to assess the model's performance in predicting AS severity and to determine the optimal cut-off point.

Results: The SIC emerged as a significant predictor of AS severity, with an odds ratio (OR) of 0.021 [95% confidence interval (CI): 0.004–0.295, P=0.008]. Incorporating SIC into a model alongside standard echocardiographic parameters notably enhanced the C-statistic/ROC area from 0.7023 to 0.8083 (P=0.01).

Conclusions: The SIC, serving as an additional echocardiography-based marker, shows promise in enhancing AS severity detection.

Keywords: Aortic stenosis (AS); calcification; echocardiography; signal intensity coefficient (SIC)

Submitted Apr 23, 2024. Accepted for publication Nov 04, 2024. Published online Dec 16, 2024.
doi: 10.21037/cdt-24-179
View this article at: https://dx.doi.org/10.21037/cdt-24-179

Introduction

Echocardiography serves as the standard imaging method for aortic stenosis (AS) severity assessment. It utilizes two-dimensional imaging and Doppler techniques to evaluate parameters such as the mean transvalvular gradient, maximum aortic jet velocity (V_{max}), dimensionless index (DI), and aortic valve area (AVA) calculated using the continuity equation (1,2). Despite its validation against invasive measures, discrepancies in echocardiographic data due to methodological differences, left ventricular

outflow tract (LVOT) measurement variability (smaller LVOT diameter can lead to overestimation of AS severity), the pressure recovery phenomenon, and flow state conditions may necessitate additional modalities, such as transesophageal echocardiography, computed tomography (CT) scans, magnetic resonance imaging (MRI), or cardiac catheterization for accurate assessment (3-9). However, the clinical application of these additional modalities is limited by factors such as time consumption, restricted access, and potential adverse effects of contrast agents.

The signal intensity coefficient (SIC) in echocardiography, which measures the reflectivity of ultrasound waves from different heart tissues, has been proposed as a potential tool for identifying the presence and severity of AS (10). Unlike machine learning approaches, this method bypasses the need for extensive labeled datasets, aiming for automated calcium detection and quantification to streamline AS assessment. This entails applying an adaptive image threshold technique for segmenting images, resulting in a binary image where calcium regions appear white and other anatomical structures appear black. The aim is to accurately detect aortic valve calcification while measuring pixel intensity and the count of white pixels, both indicative of calcium quantity. Higher SIC values indicate greater reflectivity of ultrasound waves, suggesting the presence of more calcium.

The aim of this study was to evaluate the potential of a novel echocardiography-based marker, the SIC, for identifying and quantifying calcium in AS, addressing the need for more accurate noninvasive diagnostic methods. We present this article in accordance with the STROBE reporting checklist (available at https://cdt.amegroups.com/article/view/10.21037/cdt-24-179/rc).

Highlight box

Key findings

- Signal intensity coefficient (SIC) was found to be a significant predictor of aortic stenosis (AS) severity.
- Incorporating SIC with standard echocardiographic parameters significantly improved the C-statistic/receiver operating characteristic (ROC) area.
- SIC is a promising additional echocardiography-based marker that can enhance the detection and quantification of AS severity.

What is known and what is new?

- Echocardiography is a widely used tool for assessing AS and has been validated against invasive measurements. However, discrepancies in the data can arise, leading to uncertainty about the true severity of AS and potentially requiring additional diagnostic procedures. This highlights the need for improved noninvasive diagnostic methods.
- The SIC proved to be a significant predictor of AS severity, with an odds ratio of 0.021 (95% confidence interval: 0.004–0.295, P=0.008). When incorporated into a model with standard echocardiographic parameters, the SIC significantly improved the ROC area from 0.702 to 0.808 (P=0.01).

What is the implication, and what should change now?

- The SIC, as an additional echocardiography-based marker, shows promise in enhancing the detection of AS severity. It is potentially a useful addition for software to be incorporated into echocardiographic machines and reading stations, and may be the basis for further research.

Methods

Study methods

Between May 2022 and October 2023, we retrospectively queried our database and retrieved patients initially referred to our institution's specialty clinic for AS evaluation. For this study we focused on a group of 200 adult patients diagnosed with confirmed severe AS and a group of 85 adult patients with mild or moderate AS, both at the Eastern Slovak Institute of Cardiovascular Diseases and School of Medicine, Pavol Jozef Safarik University, Kosice, Slovakia. To be included in the study, patients had to meet specific criteria, including confirmed AS, being over 18 years of age, and being in sinus rhythm. Patients with atrial fibrillation, storage or infiltrative disorders, other significant valve diseases affecting hemodynamics, implantable devices, systemic hypertension or poor echocardiographic windows were excluded. Thus, our final population comprised 162 patients (112 with severe AS, 50 with mild or moderate AS). Details of patients enrollment are listed in *Figure 1*. All patients included were informed about their participation, they had given the option to opt out and all of them provided written informed consent to participate in the study. The study was conducted in accordance with the Declaration of Helsinki (as revised in 2013) and received approval from the local ethics committee of Eastern Slovak Institute of Cardiovascular Diseases and School of Medicine, Pavol Jozef Safarik University, Kosice, Slovakia (IRB/ERC:2771-343).

Routine echocardiographic analysis

Echocardiographic scans were conducted using a SC 2000

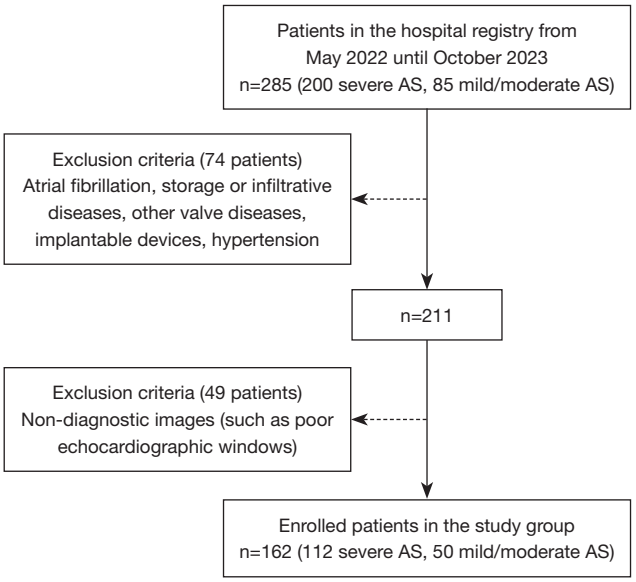

Figure 1 Flowchart of patients enrollment. AS, aortic stenosis.

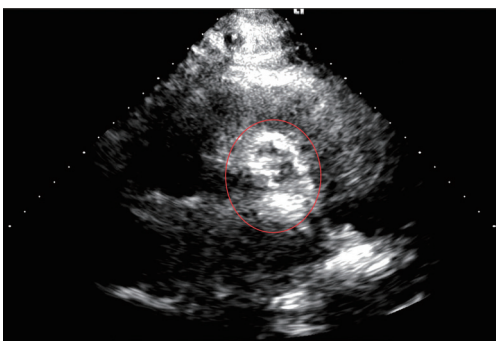

Figure 2 Echocardiography image with CLAHE—the red circle highlights the region of interest where the calcified aortic valve is located. CLAHE, Contrast Limited Adaptive Histogram Equalization.

Prime ultrasound system (Siemens Healthineers, Erlangen, Germany). The standard 2D echocardiography protocol encompassed all standard views, incorporating pulsed Doppler for left ventricular outflow tract assessment and continuous aortic Doppler flow from apical and modified right parasternal views. The AVA was determined using the continuity equation. Standard echocardiographic criteria were employed to identify severe AS (11,12):

- V_{max} >4 m/s;
- Mean gradient (MG) >40 mmHg;
- DI ≤0.25;
- AVA by continuity equation ≤1 cm^2.

As a mild or moderate AS were considered patients with following echocardiographic measures (11,12):

- V_{max} ≤4 m/s;
- MG ≤40 mmHg;
- DI >0.25;
- AVA by continuity equation >1 cm^2.

Echocardiographic tissue analysis

To analyze tissue characteristics within a specific region of interest (ROI), we employed a computational image analysis technique implemented on the ImageJ software platform v1.51, developed by the National Institutes of Health in Bethesda, Maryland, USA (13,14). This method was applied to transthoracic echocardiographic images obtained via B-mode imaging using a parasternal short-axis view. The end-diastolic frame, providing clear visualization of the entire aortic annulus and leaflet tips, was chosen for analysis.

Subsequently, the "plot profile" function in the "Analyze" drop-down menu was utilized to generate a histogram illustrating the gray value on the y-axis and distance in pixels on the x-axis. In the first stage, the image histogram was equalized to enhance contrast and extend the intensity range using the "equalizeHist" function. This equalization maps one distribution to another, creating a more uniform and wider distribution of pixel intensity values, effectively spreading the intensities across the entire range. With pixel grayscale intensities ranging from 0 to 255, the new intensity values of the equalized image are obtained by applying the following remapping function to the source echocardiography image. Subsequently, to further enhance the contrast of the equalized image, a Contrast Limited Adaptive Histogram Equalization (CLAHE) algorithm was implemented (15). This algorithm divides the image into several non-overlapping regions of nearly equal size, creating multiple histograms that redistribute the image brightness, thereby improving the overall image contrast. Finally, an image binarization technique was applied using a fixed threshold of 140 on the pixel grayscale value (ranging from 0 to 255) (16). Pixels with intensities above 140 were converted to white [255], and the remaining pixels were converted to black [0], aiding in the identification of regions with calcium presence (*Figure 2*). To address natural noise constraints in echocardiography imaging, particularly from sampling still images from echocardiography videos, various blurring treatments were applied. These treatments helped reduce image noise caused by echocardiography

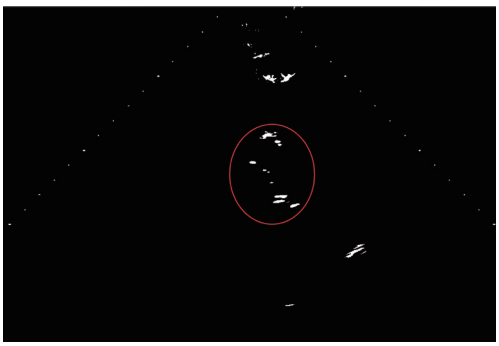

Figure 3 Binarization of an echocardiography image—the red circle represents our region of interest (aortic valve).

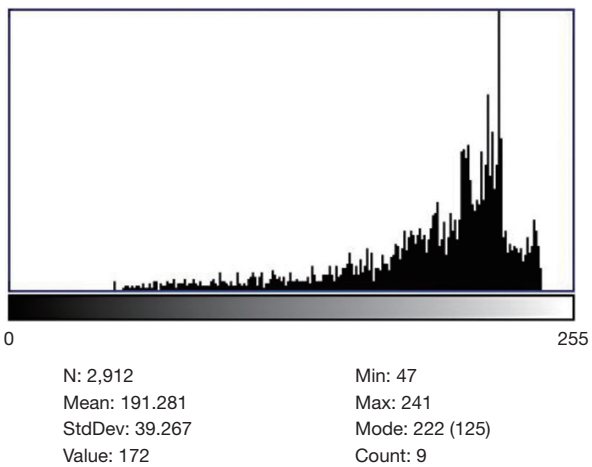

Figure 4 The signal intensity coefficient value is determined by examining the distribution of signal intensity values obtained from the region of interest, which are represented along a standard gray scale. StdDev, standard deviation.

motion. Blurring the image averages rapid changes in pixel intensities, acting as a low-pass filter that removes noise while preserving most of the image structures.

To identify calcium, we needed to determine a threshold for image segmentation, resulting in a binarized image where the foreground (calcium regions) is white (*Figure 3*). We initially used a constant threshold of 160 for the pixels. Pixel values above this threshold were classified as calcium, while those below it were considered non-calcium (such as blood, fat, muscle, or fibrous tissue). This initial constant threshold was established and validated in previous studies (10). Regions identified as calcium, with intensities above the dynamic threshold, allowed for counting the number of white pixels. This count serves as a proxy for the region's area and provides an indication similar to the calcium score identified by a CT scan.

As the last step, by clicking the "List" button at the bottom left of the histogram, a numerical table of "Plot Values" was obtained, representing the mean pixel intensities at various points along the tissue waveform (*Figure 4*). The 25th percentile of the signal intensity distribution (p) was computed. The SIC was then calculated using the formula SIC =1-p/256. This SIC measure serves as an indicator of aortic valve microstructure, capturing changes in its tissue resulting from the interaction of the ultrasound signal across the maximum thickness of the valve. In this study, the ImageJ algorithm was utilized to quantify the SIC measure from echocardiographic images of all participants while maintaining blinding to their gradient and clinical status. Previous studies have reported correlation coefficients of 0.89 and 0.90 for inter-reader and intra-reader reproducibility of SIC, respectively (16-19).

Statistical analysis

Continuous variables are presented as mean ± standard deviation (SD) if normally distributed, or as median and interquartile range if non-normally distributed. Categorical variables are presented as counts and percentages. Bivariate analysis was conducted using appropriate statistical tests based on variable nature: the two-sided *t*-test or the Wilcoxon rank-sum test (Mann-Whitney *U* test) for continuous variables, and the Chi-square test for independence or Fisher's exact test for categorical variables. Multivariate analysis utilized logistic regression, employing variable selection methods such as backward elimination and stepwise, considering the small sample size. Receiver operator characteristic (ROC) curves were used to evaluate the performance of different models in predicting AS severity and to identify its best cut-off. The SIC cutoff value (threshold) for dichotomization to determine severe AS was evaluated using the two-sample *t*-test, simple logistic regression, and sensitivity analysis. A two-tailed P value <0.05 was considered statistically significant. Statistical analysis was carried out using Prism 9.3.0 (GraphPad Software, San Diego, California, USA).

Results

A total of 162 study subjects participated, comprising 112 individuals diagnosed with severe AS and 50 patients with mild or moderate AS confirmed via transthoracic

Table 1 Clinical and echocardiographic characteristics of patients with and without echocardiography proven severe aortic stenosis

Covariate	Severe AS (n=112)	Mild or moderate AS (n=50)	P value	Odds ratio or difference between two means (95% CI)
Age (years)	78.96±7.73	73.82±6.91	0.04	5.14 (2.75, 7.53)
Male gender	59 (52.68)	28 (47.32)	0.37	0.875 (0.80, 1.04)
LVEF (%)	52.27±8.37	57.73±6.14	0.048	−5.46 (−7.76, −3.16)
BSA (m^2)	1.87±0.21	1.68±0.19	0.03	0.19 (0.12, 0.26)
V_{max} (m/s)	4.52±0.57	3.17±0.42	0.04	1.35 (1.19, 1.51)
MG (mmHg)	49.84±8.95	29.15±6.4	0.04	20.69 (18.26, 23.12)
DI	0.19±0.05	0.32±0.06	0.04	−0.13 (−0.15, −0.11)
AVA (cm^2)	0.66±0.19	1.56±0.45	0.02	−0.9 (−1.03, −0.77)
SIC	0.39±0.12	0.18±0.05	0.01	0.21 (0.18, 0.24)

Data are presented as n (%) or mean ± SD. Severe aortis stenosis was defined as: V_{max} >4 m/s, MG >40 mmHg, DI ≤0.25, and AVA by continuity equation ≤1 cm^2. Mild and moderate were defined as: V_{max} ≤4 m/s, MG ≤40 mmHg, DI >0.25, AVA by continuity equation >1 cm^2. LVEF, left ventricular ejection fraction; BSA, body surface area; V_{max}, maximum aortic jet velocity; MG, mean gradient; DI, dimensionless index; AVA, aortic valve area; SIC, signal intensity coefficient; AS, aortic stenosis; CI, confidence interval; SD, standard deviation.

Table 2 A multivariate logistic regression analysis performed using the backward elimination method to select the variables for inclusion in the model

Parameter	Estimate	Standard error	Chi-square test statistics	P value	OR (95% CI)
Intercept	4.5253	1.7933	8.8051	0.004	–
AVA (cm^2)	1.3034	0.6475	7.1939	0.007	9.357 (1.115, 58.643)
SIC	−3.6259	1.6009	6.923	0.008	0.021 (0.004, 0.295)

Statistical tests used: OR for male gender: Fisher's exact test; 95% CI for differences in means: two-sample *t*-test. AVA, aortic valve area; SIC, signal intensity coefficient; OR, odds ratio; CI, confidence interval.

echocardiography. No significant differences in age and gender were observed across all groups (*Table 1*). Among the assessed echocardiographic parameters, statistically significant disparities were noted for body surface area (BSA), V_{max}, DI, and AVA. Notably, the most significant discrepancy was observed in AVA mean difference of −0.9 [95% confidence interval (CI): −1.03, −0.77]. *Table 1* also depicted the mean values ± SD for the SIC in patients with and without severe AS, where a statistically significant mean difference in SIC (0.21, 95% CI: 0.18 to 0.24, P=0.01) was evident.

A multivariate logistic regression analysis was conducted to predict severe AS, incorporating traditional and new variables, including age, sex, left ventricular ejection fraction (LVEF), BSA, V_{max}, MG, DI, AVA, and SIC. However, no convergent results were obtained, and none of the predictors (excluding LVEF) were deemed significant. Subsequent separate multivariate analyses focusing solely on traditional variables or the two new variables similarly failed to identify any significant predictors, potentially due to multicollinearity. Nonetheless, employing variable selection methods consistently identified two significant predictors: traditional AVA (OR: 9.357, 95% CI: 1.115–58.643, P=0.007) and the new variable SIC (OR: 0.021, 95% CI: 0.004–0.295, P=0.008), as summarized in *Table 2*.

Table 3 summarizes the results, including estimated ROC area, standard error, and 95% CI through bootstrap sampling. While the multivariate logistic regression model using only traditional AVA exhibited modest predictive performance (ROC area: 0.7023, 95% CI: 0.5476–0.857), the model incorporating both AVA and SIC demonstrated superior performance (ROC area: 0.8083, 95% CI: 0.6893–0.9274), outperforming other variable subsets. It's worth mentioning that dichotomizing AS as severe or non-

Table 3 The performance of different models in predicting severity of aortic stenosis compared using ROC curve area estimates

Parameter	ROC area	Standard error	95% confidence limits
AVA	0.7023	0.0978	0.5476–0.857
SIC and AVA	0.8083	0.0749	0.6893–0.9274

Different models are identified by the subsets of the predictors in the first column. The model in the bottom row which includes the predictor AVA is the reference model. ROC, receiver operating characteristic; AVA, aortic valve area; SIC, signal intensity coefficient.

severe based on standard echocardiographic numerical measures is a commonly adopted approach.

In the overall study population, significant correlations were observed between SIC and both V_{max} (r=0.48, P<0.01) and AVA (r=–0.62, P<0.01). Pearson correlation between SIC and MG was 0.70, and between SIC and DI was 0.57 (*Figure 5*).

Discussion

The aim of this pilot study was to assess whether a novel echocardiography-based measure could aid in identifying alterations in the tissue structure of the aortic valve in AS patients. Our results reveal a significant correlation between echocardiographic SIC values and established indicators of AS severity, including V_{max}, AVA, DI, and MG. This suggests that an elevated SIC reflects physiological changes leading to structural modifications in valve leaflets and increased hemodynamic stress. Thus, our findings suggest that echocardiographic SIC, akin to echocardiography-based quantification of AS severity, offers valuable insights into subtle abnormalities in aortic valve composition across different disease states, although the clinical applications of SIC require further investigation.

AS is a progressive condition characterized by the thickening and stiffening of the heart valve, leading to blockage of the valve opening. The development of AS involves a cycle of calcification, valve injury, and subsequent calcification, which is the focus of advanced imaging techniques and medical interventions. The aortic valve is composed of three flexible leaflets made of collagen fibers and two main cell types: valvular endothelial cells and valvular interstitial cells. These leaflets are designed to endure the stresses of blood flow throughout a person's lifetime. However, in AS, the leaflets gradually thicken and calcify, resulting in obstruction in the left ventricular outflow tract. AS progresses through two distinct stages: initiation, akin to atherosclerosis, and propagation, marked by calcification and fibrosis driving disease advancement. These phases may coexist variably within the valve. Emerging imaging modalities and therapies aim to target the cycle of leaflet calcification, valve injury, and subsequent calcification (20). Endothelial damage, triggered by repetitive mechanical stress on the valve, initiates AS. Individuals with bicuspid aortic valves are particularly prone to this damage. Inflammatory cells, including macrophages and oxidized LDL, infiltrate and form microcalcifications near lipid deposition sites, mirroring atherosclerosis. Cardiovascular risk factors such as age, smoking, hypertension, hyperlipidemia, and diabetes are associated with AS incidence, though risk factors for disease progression may differ (21). Transitioning valvular interstitial cells into osteoblastic phenotype marks the progression from initiation to propagation phases. Osteoblast-like cells contribute to disease advancement by creating a feedback loop, promoting further calcification.

The application of SIC and other ultrasound measures for evaluating myocardial microstructure has been explored in various cardiac disease phenotypes, such as aortic dissection, heart failure, immune-inflammatory disease, metabolic syndrome, hypertensive heart disease, diabetic cardiomyopathy, and myocardial infarction (22-27). Previous research methodologies have been limited by reliance on non-human models, retrospective designs, or use of integrated or mean values of backscatter signal intensities (22,23,28). In contrast, SIC leverages the entire grayscale distribution of the ultrasonic signal to provide information about tissue microstructure. Furthermore, utilizing end-diastolic B-mode frames helps mitigate signal reconstruction artifacts (23).

Shifts in signal intensity distribution, as captured by the SIC measure, seem to mirror tissue-level changes, including myocardial hypertrophy, increased myocyte density, and collagen deposition (29-31). Therefore, variations in SIC, although measured in a predefined ROI of the aortic valve, may represent diffuse tissue-level alterations characteristic of AS. Our findings suggest that SIC could serve as a noninvasive measure of aortic valve changes in AS individuals. While SIC may predominantly reflect leaflet calcifications in the context of AS, it could also encompass a range of other tissue-level changes. Hence, the combined use of SIC and echocardiography, obtained through different imaging techniques, could complementarily

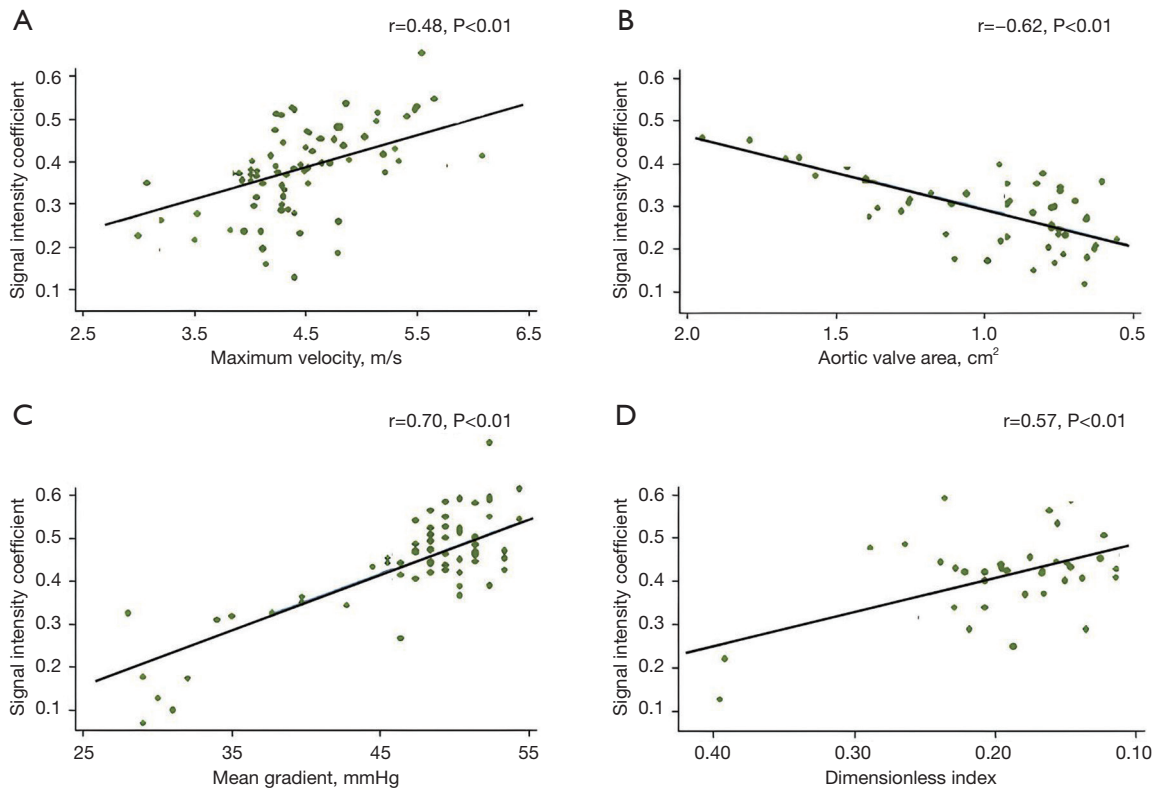

Figure 5 Associations of the signal intensity coefficient with maximum velocity (A), aortic valve area (B), mean gradient (C), and dimensionless index (D).

assess AS progression and provide crucial disease-related information as a future concept for reducing radiation usage. However, further research is needed to fully evaluate the diagnostic and prognostic potential of SIC using echocardiography.

Study limitations

There are several limitations in our study that should be taken into consideration. Firstly, our conclusions are based on a single-center study design, which involved a small number of participants. This may introduce patient selection bias and limit the generalizability of our findings. In a retrospective study design, the timing of echocardiography can vary slightly between cases. Secondly, we did not determine the Agatston score in this study, which could serve as a useful indicator of AS severity and potentially be correlated with SIC (32). Furthermore, we did not utilize the gold standard method of assessing AS severity, which is cardiac catheterization incorporating gradients, cardiac output measurements, and the assessment of tricuspid regurgitation, which can impact accuracy. It is also important to note that echocardiography is at best a semi-quantitative method and has a very high degree of inter-examiner variability. Moreover, SIC values may also be affected by factors such as the angle of incidence of the ultrasound waves, the depth of the tissue being imaged, and the quality of the imaging equipment (33). Finally, in order to consider our results as generalizable and fully understand how SIC can be used to monitor disease progression, it is necessary to validate and expand upon our findings through longitudinal studies involving larger and more diverse groups of patients.

Conclusions

Our study results suggest that echocardiographic SIC offers a noninvasive method to detect early alterations in the composition of the aortic valve, akin to echocardiography-based quantification of AS. This introduces an easily accessible imaging tool for assessing tissue-level changes in AS, supplementing traditional echocardiography and CT

measurements. Our work could be a good start into a new diagnostic tool with the potential to reduce radiation by eliminating the need for diagnostic CT as a golden standard before aortic valve replacement. Nevertheless, additional research is warranted to elucidate the connection between SIC variations and specific tissue-level changes in AS. Longitudinal studies are also essential to assess the potential of SIC as a dependable marker of disease progression or response to AS treatments.

Acknowledgments

The authors would like to acknowledge the support staff for its timely effort, sincerity, and dedication towards work.
Funding: This study was funded by the EU NextGenerationEU through the Recovery and Resilience Plan of the Slovak Republic within the project No. 09I03-03-V05-00008, and by Pavol Jozef Safarik University through grant VVGS ESGV: vvgs-2023-2917.

Footnote

Reporting Checklist: The authors have completed the STROBE reporting checklist. Available at https://cdt.amegroups.com/article/view/10.21037/cdt-24-179/rc

Data Sharing Statement: Available at https://cdt.amegroups.com/article/view/10.21037/cdt-24-179/dss

Peer Review File: Available at https://cdt.amegroups.com/article/view/10.21037/cdt-24-179/prf

Conflicts of Interest: All authors have completed the ICMJE uniform disclosure form (available at https://cdt.amegroups.com/article/view/10.21037/cdt-24-179/coif). The authors have no conflicts of interest to declare.

Ethical Statement: The authors are accountable for all aspects of the work in ensuring that questions related to the accuracy or integrity of any part of the work are appropriately investigated and resolved. The study was conducted in accordance with the Declaration of Helsinki (as revised in 2013) and received approval from the local ethics committee of Eastern Slovak Institute of Cardiovascular Diseases and School of Medicine, Pavol Jozef Safarik University, Kosice, Slovakia (IRB/ERC:2771–343). All patients included were informed about their participation, they had given the option to opt out and all of them provided written informed consent to participate in the study.

References

1. Pibarot P. Discordant Low-Gradient Aortic Stenosis: Assessing the Valve and the Myocardium. Tex Heart Inst J 2024;51:e238288.
2. Baumgartner H, Hung J, Bermejo J, et al. Recommendations on the Echocardiographic Assessment of Aortic Valve Stenosis: A Focused Update from the European Association of Cardiovascular Imaging and the American Society of Echocardiography. J Am Soc Echocardiogr 2017;30:372-92.
3. Chandrasekar B, Panchadar S, Almerri K, et al. Pre-discharge (18)F-Flourodeoxyglucose uptake pattern following transcatheter aortic-valve replacement and adverse prognostic features in aortic stenosis. Indian Heart J 2023;75:386-9.
4. Tastet L, Vincent F, Pibarot P. Cardiac Damage Staging in Aortic Stenosis: A Perspective From the Cardiac Catheterization Laboratory. Can J Cardiol 2020;36:1583-6.
5. Troger F, Tiller C, Reindl M, et al. Slice positioning in phase-contrast MRI impacts aortic stenosis assessment. Eur J Radiol 2023;161:110722.
6. Choe J, Koo HJ, Choi SJ, et al. Differences in aortic valve area measured on cardiac CT and echocardiography in patients with aortic stenosis. PLoS One 2023;18:e0280530.
7. Michelena HI, Margaryan E, Miller FA, et al. Inconsistent echocardiographic grading of aortic stenosis: is the left ventricular outflow tract important? Heart 2013;99:921-31.
8. Clavel MA, Ennezat PV, Maréchaux S, et al. Stress echocardiography to assess stenosis severity and predict outcome in patients with paradoxical low-flow, low-gradient aortic stenosis and preserved LVEF. JACC Cardiovasc Imaging 2013;6:175-83.
9. Bradley SM, Foag K, Monteagudo K, et al. Use of routinely captured echocardiographic data in the diagnosis

of severe aortic stenosis. Heart 2019;105:112-6.
10. Elvas LB, Almeida AG, Rosario L, et al. Calcium Identification and Scoring Based on Echocardiography. An Exploratory Study on Aortic Valve Stenosis. J Pers Med 2021;11:598.
11. Stassen J, Ewe SH, Pio SM, et al. Managing Patients With Moderate Aortic Stenosis. JACC Cardiovasc Imaging 2023;16:837-55.
12. Jhun CS, Newswanger R, Cysyk JP, et al. Dynamics of Blood Flows in Aortic Stenosis: Mild, Moderate, and Severe. ASAIO J 2021;67:666-74.
13. Hiremath P, Lawler PR, Ho JE, et al. Ultrasonic Assessment of Myocardial Microstructure in Hypertrophic Cardiomyopathy Sarcomere Mutation Carriers With and Without Left Ventricular Hypertrophy. Circ Heart Fail 2016;9:10.1161/CIRCHEARTFAILURE.116.003026 e003026.
14. Hiremath P, Bauer M, Aguirre AD, et al. Identifying early changes in myocardial microstructure in hypertensive heart disease. PLoS One 2014;9:e97424.
15. Reza AM. Realization of the Contrast Limited Adaptive Histogram Equalization (CLAHE) for Real-Time Image Enhancement. J Signal Process Syst 2014;38:35-44.
16. Michalak H, Okarma K. Improvement of Image Binarization Methods Using Image Preprocessing with Local Entropy Filtering for Alphanumerical Character Recognition Purposes. Entropy (Basel) 2019;21:562.
17. Niblack W. An Introduction to Digital Image Processing. Prentice Hall: Englewood Cliffs, NJ, USA; 1986.
18. Sauvola J, Pietikäinen M. Adaptive document image binarization. Pattern Recognit 2000;33:225-36.
19. Wolf C, Jolion JM. Extraction and recognition of artificial text in multimedia documents. Form Pattern Anal Appl 2004;6:309-26.
20. Pawade T, Sheth T, Guzzetti E, et al. Why and How to Measure Aortic Valve Calcification in Patients With Aortic Stenosis. JACC Cardiovasc Imaging 2019;12:1835-48.
21. Stritzke J, Linsel-Nitschke P, Markus MR, et al. Association between degenerative aortic valve disease and long-term exposure to cardiovascular risk factors: results of the longitudinal population-based KORA/MONICA survey. Eur Heart J 2009;30:2044-53.
22. Nguyen CT, Hall CS, Wickline SA. Characterization of aortic microstructure with ultrasound: implications for mechanisms of aortic function and dissection. IEEE Trans Ultrason Ferroelectr Freq Control 2002;49:1561-71.
23. Kwan A, Demosthenes E, Salto G, et al. Cardiac microstructural alterations measured by echocardiography identify sex-specific risk for heart failure. Heart 2022;108:1800-6.
24. Kwan AC, Nguyen T, Kim EH, et al. Ultrasonic Texture Analysis Identifies Cardiac Microstructural Alterations in Immune-Inflammatory Disease. medRxiv 2023. doi: 10.1101/2020.06.10.20125443.
25. Ho JE, Rahban Y, Sandhu H, et al. Preclinical Alterations in Myocardial Microstructure in People with Metabolic Syndrome. Obesity (Silver Spring) 2017;25:1516-22.
26. Di Bello V, Talarico L, Picano E, et al. Increased echodensity of myocardial wall in the diabetic heart: an ultrasound tissue characterization study. J Am Coll Cardiol 1995;25:1408-15.
27. Barzilai B, Thomas LJ 3rd, Glueck RM, et al. Detection of remote myocardial infarction with quantitative real-time ultrasonic characterization. J Am Soc Echocardiogr 1988;1:179-86.
28. Mizuno R, Fujimoto S, Saito Y, et al. Non-invasive quantitation of myocardial fibrosis using combined tissue harmonic imaging and integrated backscatter analysis in dilated cardiomyopathy. Cardiology 2007;108:11-7.
29. Li S, Zhao L, Zhang B, et al. Ultrasound cardiogram-based diagnosis of cardiac hypertrophy from hypertension and analysis of its relationship with expression of autophagy-related protein. Ann Palliat Med 2022;11:684-94.
30. Villemain O, Baranger J, Friedberg MK, et al. Ultrafast Ultrasound Imaging in Pediatric and Adult Cardiology: Techniques, Applications, and Perspectives. JACC Cardiovasc Imaging 2020;13:1771-91.
31. Han R, Yan Y, Ding Y, et al. The Correlation Between Collagen Types and Ultrasound Feature Score in Evaluating the Vulnerability of Carotid Artery Plaque. Front Cardiovasc Med 2021;8:756424.
32. Wang TKM, Flamm SD, Schoenhagen P, et al. Diagnostic and Prognostic Performance of Aortic Valve Calcium Score with Cardiac CT for Aortic Stenosis: A Meta-Analysis. Radiol Cardiothorac Imaging 2021;3:e210075.
33. Hiremath P, Bauer M, Cheng HW, et al. Ultrasonic assessment of myocardial microstructure. J Vis Exp 2014;(83):e50850.

Cite this article as: Poruban T, Pella D, Schusterova I, Jakubova M, Sieradzka Uchnar KA, Barbierik Vachalcova M. A computer vision model for the identification and scoring of calcium in aortic valve stenosis: a single-center experience. Cardiovasc Diagn Ther 2024;14(6):1029-1037. doi: 10.21037/cdt-24-179

